Separability of multiple deep crack defects with an NDE Eddy Current System

Rimond Hamia, Christophe Cordier, Christophe Dolabdjian

Separability of Multiple Deep Crack Defects With an NDE Eddy Current System

R. Hamia, C. Cordier, and C. Dolabdjian

GREYC UMR 6072-University of Caen Basse Normandie and ENSICAEN 14050 Caen Cedex, France

Finite element simulation was carried out to characterize the separability of an eddy current nondestructive testing (EC-NDT) system in the case of the detection of deep cracks located in an aluminum plate. The interaction among multiple cracks was also analyzed. The results show that the separability of the EC system not only depends on the sensitive element dimensions but also on different parameters of the system, such as the sensor lift-off, the excitation frequency and the cracks depth. Furthermore, the simulations show that under some conditions, the magnetic response sensed for multiple cracks can be calculated as the superposition of the signals obtained for each crack. This point essentially simplifies the solution of the inverse problem of crack reconstruction.

***Index Terms*—Eddy current testing (ECT), magnetometer, multiple cracks and spatial resolution, nondestructive testing (NDT).**

I. Introduction

THE USE of high sensitivity magnetic sensors in EC-NDT systems leads to improve the detection performances of deep cracks. In recent years, different kinds of magnetometers were implemented and tested in EC-NDT state of art system, like SQUID [1], Flux-gates [2], Hall sensors [3], GMI [4], and GMR [5]. The state of the art studies shows contribution of these technologies in the detection of deep cracks by ECT. Nevertheless, the development of these systems was often done by taking into account only one point of the detection system, for example the properties of the sensor element. In fact, to improve the detection performances (detection depth, Signal to Noise Ratio, spatial resolution. . .) of any EC-NDT system, it is first of all necessary to have a complete vision of the measurement problem and we should take into account the whole system as described in Fig. 1.

Fig. 1 provides an overview of the different relationships between the detection performances and the parameters of the EC-NDT system (inducer, sensor, environment, and plate properties). Among these parameters, only the parameters related to the detection instrument (sensor and inducer) can be adjusted to achieve a system able to detect deep cracks in the best measurement conditions.

To analyze and optimize the performances detection of an EC-NDT system, we have adopted in previous work a meticulous methodology which consists in introducing a systemic approach that includes all the aspects of an EC system. For example, the study of the effect of the crack size, the excitation frequency, the lift-off and the material properties, on the magnetic crack signature and the Signal to Noise Ratio has led to many enhancement and optimization for our EC-NDT system [6].

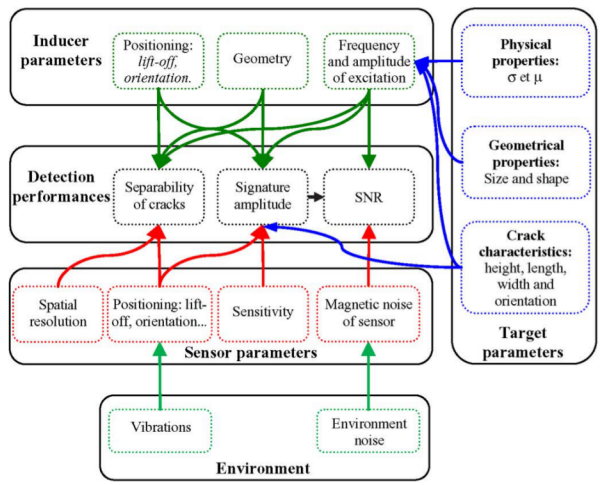

Fig. 1. Presentation of the main relationships among the different parameters of an EC-NDT system.

In this paper we pursue the detection performances enhancement of our EC-NDT system. For this reason, a 3-D-FEM model was used to predict the magnetic response from our NDT system. We study the effect of different parameters on the system capacity to separate close cracks and the interaction among multiple cracks.

This paper is organized as follows. The EC system and the numerical model are briefly presented in Section II. In Section III, the capacity of the device to separate close cracks is analyzed and studied in relation with some system parameters like the excitation frequency, the plate thickness and the lift-off. Section IV is devoted to the analysis of the interaction among multiple close cracks. This is followed by a conclusion.

II. EC-NDT System and Numerical Model

A. EC-NDT System

The NDT system used in this study is composed of a magnetometer which is built with a GMR element to sense the magnetic field. This magnetometer has very good characteristics for EC-NDT in shielded and unshielded environment for the deep cracks detection. An EC-NDT setup was used to evaluate the

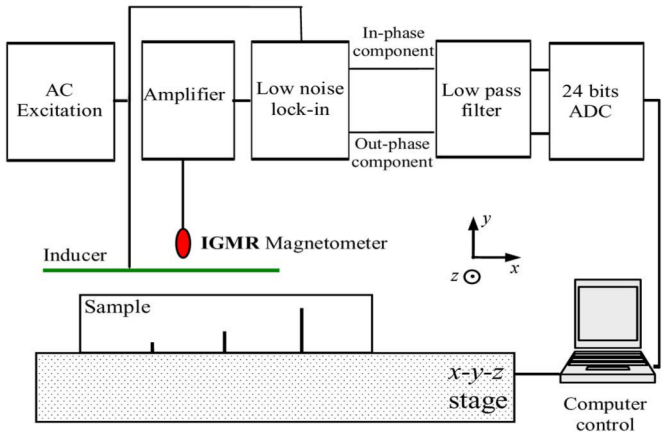

Fig. 2. Sketch view of the nondestructive evaluation implemented system.

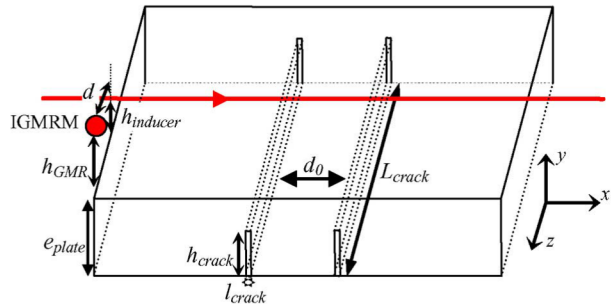

Fig. 3. Sketch view of the studied aluminum sample plate with associated subsurface cracks ($L_{\text{plate}} = 160$ mm, $l_{\text{plate}} = 50$ mm, $t_{\text{plate}} = 10$ mm, $h_{\text{inducer}} = 1$ mm, $h_{\text{GMR}} = 2$ mm, $h_{\text{crack}} = 2$ mm, $l_{\text{crack}} = 0.5$ mm, $d = 12$ mm, $\sigma = 1.68 \times 10^7$ S/m).

performances of an IGMRM [7] dedicated to the measurement of deep lying cracks in conducting materials. Fig. 2 shows the used experimental setup. It consists of the IGMRM oriented so as to detect the tangential component of magnetic field, B_x, appearing near the inducer. This latest is made of a single wire inducer which is fed by a sinusoidal current at the frequency, f_{exc}, and an amplitude, I. More details of this system and the advantages of using this kind of inducer are given in previous papers [6].

The performances of this instrument were previously studied and compared to classical ones. This IGMRM was also implemented and tested in different kinds of eddy current systems [8], [9].

B. Numerical Model

A numerical model based on the finite element method (FEM) was developed to simulate the EC-IGMRM inspection system, to analyze its performances and to predict the signal measured by the GMR sensors. We have used the edge finite element formulation $\mathrm{A}^* - \varphi_\mathrm{r}$ [10] and have implemented it in Comsol Multiphysics. The governing equations can be easily derived from Maxwell's equations and expressed as

$$\nabla \times \left[(\mu_0\mu_r)^{-1}\nabla \times A^*\right] + j\omega\sigma A^* = 0, \quad \text{in conducting region,} \tag{1}$$

$$\nabla \cdot [\mu_0 \nabla \varphi_r] = 0, \text{ in nonconducting region} \tag{2}$$

where $\boldsymbol{A}^*$ is the modified magnetic vector potential solved in the conducting region and φ_r the reduced magnetic scalar potential solved in the region of free space and source current.

This model has been already validated by comparing numerical and experimental results obtained in the case of deep cracks detection in a reference sample [6].

III. Separabitliy of Multiple Cracks Study

The separability of multiple cracks is an important factor in the performances detection analysis of an EC-NDT system. We usually mix up the spatial resolution of the system and its capacity to separate the magnetic responses of close cracks. In fact, the separability of an EC-NDT not only depends on the spatial resolution of the used sensor but also on the system parameters like the lift-off, the excitation frequency and the cracks and inducer geometry.

A. Separation of Close Cracks

The capacity of our system to distinguish two close cracks was determined by simulation. An aluminum sample plate with two identical cracks separated by a distance d_0 was studied. Fig. 3 is a schematic view of the measurement configuration used and the geometry of the plate and cracks. The geometry of the problem is discretized with tetrahedral elements and a numerical simulation is performed by the PARDISO solver with two quad-core processors (Intel Xeon X5472 at 3 GHz) and 64 GB of RAM. The CPU time needed to solve the problem is around 600 s.

The calculations were performed with and without cracks in order to evaluate the useful magnetic response induced by crack $|B_x|$ which is defined by

$$|\Delta B_x| = |B_{x,crack} - B_{x,0}| \tag{3}$$

where, $B_{x,crack}$ and $B_{x,0}$ are the magnetic flux density, sensed along the x-axis, at the magnetometer location, with and without cracks, respectively.

The detected magnetic signature of the two cracks versus the direction x of the scan is plotted in Fig. 4 for various values of the distance, d_0 (38, 20, 18, and 10 mm, respectively).

First, the results show that the proposed EC-NDT system is able to easily detect a crack at a depth 8 mm from the surface, even if the lift-off is high (2 mm, as given in Fig. 3). Moreover, the results show that for $d_0 = 38$ mm, the magnetic signature of each defect is detectable even if there is some cross-talk between cracks. When d_0 decreases, the amplitude of the two central peaks decreases and the amplitude of the two sides peaks increases. If the amplitude of central peaks is below a certain threshold, then it is impossible to know whether the magnetic signature corresponds to one or more cracks. According to these simulations, the minimum distance between cracks, $d_{0,m}$, that allows to separate the magnetic responses of two cracks is in order of 18 mm.

This distance $d_{0,m}$, for a tested sample plate with 10 mm as thickness, is relatively large knowing that the used magnetometer is considered as a punctual sensor in the context of these measurements [10]. Therefore, the separability of an EC-NDT

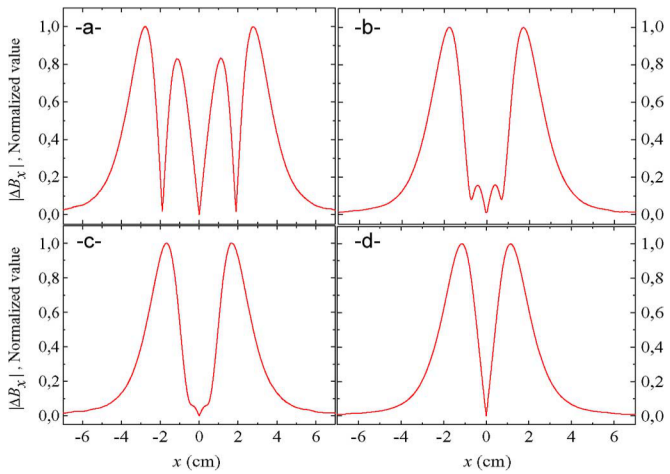

Fig. 4. Evolution of the measured signal for two deep cracks separated by the distance d_0. The normalized signal is presented in four cases: (a) $d_0 = 38$ mm, (b) $d_0 = 20$ mm, (c) $d_0 = 18$ mm, (d) $d_0 = 10$ mm. ($h_{\text{inducer}} = 1$ mm, $h_{\text{GMR}} = 2$ mm, $h_{\text{crack}} = 2$ mm, $l_{\text{crack}} = 0.5$ mm, $e_{\text{plate}} = 10$ mm, $f_{\text{exc}} = 325$ Hz, $d = 12$ mm).

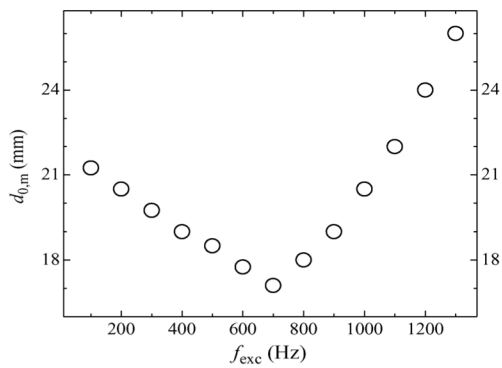

Fig. 5. Effect of the excitation frequency on the minimal distance of separation. ($h_{\text{inducer}} = 1$ mm, $h_{\text{GMR}} = 2$ mm, $h_{\text{crack}} = 2$ mm, $l_{\text{crack}} = 0.5$ mm, $e_{\text{plate}} = 10$ mm, $d = 12$ mm).

system depends on others parameters mainly the excitation frequency, the size of the inspection area and the distance between the inspection system and the cracks.

Thereafter, FEM simulations were carried out to study the effect of the excitation frequency, plate thickness and system lift-off on the system separability of multiple cracks.

B. Effect of the Excitation Frequency

To study the effect of the excitation frequency, we have calculated, for several values of f_{exc}, the distance $d_{0,m}$ separating two deep cracks in the same plate sample. The geometry and properties of the device are similar to those in Fig. 3.

Fig. 5 shows the evolution of $d_{0,\text{m}}$ as a function of excitation frequency. The simulation reveals the existence of an optimal frequency, f_{opt}, minimizing, $d_{0,m}$, the distance above which it is possible to separate two close cracks. At the frequency $f_{opt} = 700$ Hz, $d_{0,m}$ reaches a minimum value of 17 mm. Notice that this optimal frequency is not identical to the frequencies that maximize the amplitude of the signal (325 Hz) or the RSB (450 Hz) obtained in preceding work [6].

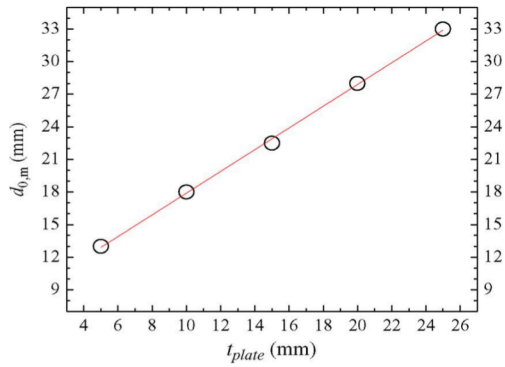

Fig. 6. Variation of $d_{0,\text{m}}$ versus the plate thickness ($d = 12$ mm, $h_{\text{inducteur}} = 1$ mm, $h_{\text{GMR}} = 2$ mm, $l_{\text{défaut}} = 0.5$ mm, $h_{\text{défaut}} = 20\%$ e_{plaque}, $f_{\text{exc}} = f_{\text{opt}}$).

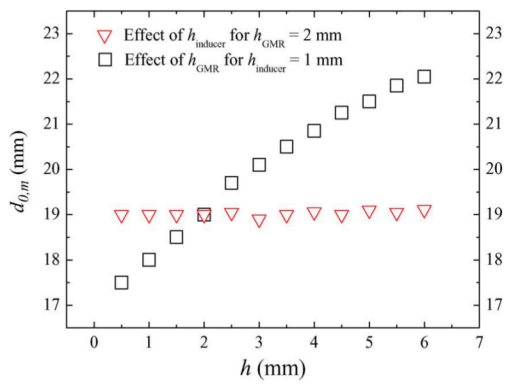

Fig. 7. Lift-off Effect of the sensor (square) and of the inducer (triangle) on the separability of the system ($h_{\text{inducer}} = 1$ mm, $h_{\text{GMR}} = 2$ mm, $h_{\text{crack}} = 2$ mm, $l_{\text{crack}} = 0.5$ mm, $f_{\text{exc}} = 325$ Hz, $d = 12$ mm).

C. Effect of the Plate Thickness and the Lift-Off

Subsequently, the effect of the plate thickness, t_{plate}, and the lift-off of the sensor and inducer were also examined. The variations of the distance, $d_{0,m}$, are respectively plotted, in Figs. 6 and 7.

Fig. 6 plots the relation between $d_{0,\text{m}}$ versus t_{plate}. The simulations were performed on plates having two cracks with the same height, h_{crack}, equal to 20% of t_{plate}. The calculations were performed using the optimal frequency, f_{opt}, for each plate thickness [6].

The results show that $d_{0,\text{m}}$ varies linearly with t_{plate} and is given by

$$d_{0,m} = 7,9 + t_{plate}\ (\text{mm}) \tag{4}$$

This increase can be explained by the combination of two effects. First, increasing the thickness of the plate leads to decrease the used optimal excitation frequency which rises the spreading of the induced current in depth. Secondly, a plate with greater thickness is accompanied by an increase in the sensor-crack distance and therefore, a wider distribution of the field lines around the sensor.

The influence of the lift-off of the sensor and the inducer on the separation capacity of our system is studied. The results are described in Fig. 7. They show that the value of the minimum distance, $d_{0,\text{m}}$, is not influenced by the variation of the inducer

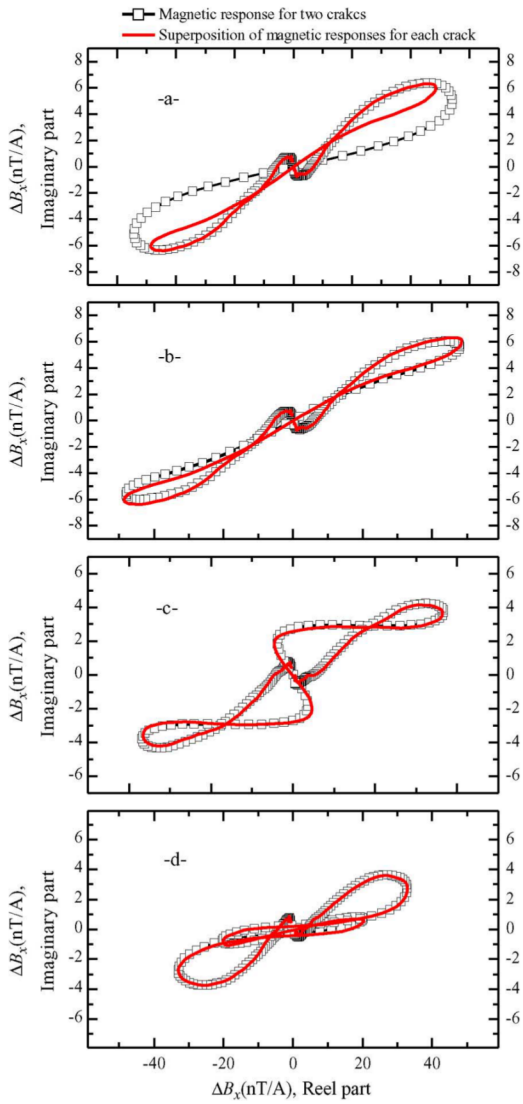

Fig. 8. Analysis of the interaction between cracks by comparing the magnetic field response for a plate having two cracks (square) and the sum of the magnetic response of each defect (solid line): (a) $d_0 = 5$ mm, (b) $d_0 = 10$ mm, (c) $d_0 = 20$ mm, (d) $d_0 = 30$ mm. ($h_{\text{inducer}} = 1$ mm, $h_{\text{GMR}} = 2$ mm, $h_{\text{crack}} = 2$ mm, $l_{\text{crack}} = 0.5$ mm, $e_{\text{plate}} = 10$ mm, $f_{\text{exc}} = 325$ Hz, $d = 12$ mm).

lift-off. However, $d_{0,m}$ almost varies linearly with the sensor lift-off because a greater lift-off leads to a wider distribution of the magnetic field sensed by the sensor. Therefore, it is suitable to use the sensor with a lift-off as small as possible in order to maximize the separation capacity of an EC-NDT system.

IV. Interaction Among Multiple Cracks

The interaction between two close cracks has been investigated using the FEM. The sensed magnetic response of two deep cracks is compared to the magnetic response obtained by the superposition of each deep crack response. The target of this study is to find the minimum distance between cracks that allows the adding of the individual cracks signals in order to get the total sensed signal.

Fig. 8 shows the Lissajous curves of the magnetic field created by two cracks in a plate. The sum of the magnetic responses of each crack is also represented.

The results show in the cases where the distance between the two cracks is greater than a limit distance ($d_0 = 5$ mm), that the magnetic signature of the defects, in terms of amplitude and phase, corresponds to the linear combination of each crack signature. Beyond this limit distance, which is less than the minimum distance of separability, $d_{0,\text{m}}$, it is interesting to note that the superposition is no longer valid. Subsequently, this aspect will be very interesting in the field of defect reconstruction in the inverse problem.

V. Conclusion

In this paper, finite element modeling was performed to study the effect of the EC system parameters on the separability of multiple deep cracks. The results show that the separation capacity mainly depends on the sensor lift-off, the excitation frequency and the distance between the sensor element and the detected crack. Furthermore, the interaction among multiple cracks was analyzed. In numerous measurement configurations, the signal can be decomposed into signals associated with individual defects. In the future, the results presented in this study will be useful in the inverse problem for crack reconstruction.

References

[1] F. Sarreshtedari, M. Hosseini, S. Razmkhah, K. Mehrany, H. Kokabi, J. Schubert, M. Banzet, H. J. Krause, and M. Fardmanesh, "Analytical model for the extraction of flaw-induced current interactions for SQUID NDE," *IEEE Trans. Appl. Supercond.*, vol. 21, no. 4, Aug. 2011.

[2] Y. Fujita and I. Sasadaa, "Detection of flaws in ferromagnetic samples based on low frequency eddy current imaging," *J. Appl. Phys., 93*, vol. 10, pp. 8277–8279, 2003.

[3] A. Sophian, G. Y. Tian, and S. Zairi, "Pulsed magnetic flux leakage techniques for crack detection and characterisation," *Sensors Actuators, A*, vol. 125, pp. 186–191, 2006.

[4] F. Vachera, F. Alvesb, and C. Gilles-Pascaud, "Eddy current nondestructive testing with giant magneto-impedance sensor," *NDT&E Int.*, vol. 40, pp. 439–442, 2007.

[5] G. Betta, L. Ferrigno, and M. Laracca, "GMR-Based ECT Instrument for detection and characterization of crack on a planar specimen: A hand-held solution," *IEEE Trans. Instr. Measur.*, vol. 61, no. 2, pp. 505–512, Feb. 2012.

[6] R. Hamia, C. Cordier, S. Saez, and C. Dolabdjian, "Eddy current non destructive testing using an improved giant magnetoresistance magnetometer and a single wire as inducer. A benchmark performance analysis with the help of the finite element method," *IEEE Trans. Magn.*, vol. 46, no. 10, pp. 3731–3737, Oct. 2010.

[7] L. Perez, C. Dolabdjian, G. Waché, and L. Butin, "Advance in magnetoresistance magnetometer performances applied in eddy current sensor arrays," presented at the 16th WCNDT'04 Conf., Montréal, QC, Canada, 28 Aug.–03 Sep. 2004.

[8] L. Perez, J. Lehir, C. Dolabdjian, and L. Butin, "Investigation in detection of fatigue cracks under rivet head airframe using improved GMR magnetometer in an Eddy Current system," *J. Electr. Eng.*, vol. 55, no. 10/s, pp. 10–11, 2004.

[9] C. Dolabdjian, G. Waché, and L. Perez, "Improvement in subsurface fatigue cracks under airframes fasteners detection using improved rotary giant magnetoresistance magnetometer head," *Insight—Non-Destructive Testing Condition Monitoring*, vol. 49, no. 2, pp. 133–136, 2007.

[10] R. Hamia, C. Cordier, S. Saez, and C. Dolabdjian, "Giant magneto impedance sensor for non destructive evaluation eddycurrent system," *Sensor Lett.*, vol. 7, no. 3, pp. 437–441, 2009.